Citation for published version:
Gonzalez-Resines, S, Quinn, PJ, Naftalin, RJ & Domene, C 2021, 'Multiple Interactions of Glucose with the Extra-Membranous Loops of GLUT1 Aid Transport', *Journal of Chemical Information and Modeling*, vol. 61, no. 7, pp. 3559-3570. https://doi.org/10.1021/acs.jcim.1c00310

DOI:
10.1021/acs.jcim.1c00310

Publication date:
2021

Document Version
Peer reviewed version

Link to publication

This document is the Accepted Manuscript version of a Published Work that appeared in final form in J. Chem. Inf. Model., copyright © American Chemical Society after peer review and technical editing by the publisher. To access the final edited and published work see https://pubs.acs.org/doi/10.1021/acs.jcim.1c00310

University of Bath

Alternative formats
If you require this document in an alternative format, please contact:
openaccess@bath.ac.uk

General rights
Copyright and moral rights for the publications made accessible in the public portal are retained by the authors and/or other copyright owners and it is a condition of accessing publications that users recognise and abide by the legal requirements associated with these rights.

Take down policy
If you believe that this document breaches copyright please contact us providing details, and we will remove access to the work immediately and investigate your claim.

Download date: 25. Jun. 2024

Multiple interactions of glucose with the extra-membranous loops of GLUT1 aid transport

Saul Gonzalez-Resines[1], Peter J Quinn[2], Richard J Naftalin[3], Carmen Domene[1,4*]*
[1]*Departments of Chemistry University of Bath*, Bath BA2 7AX, United Kingdom
[2]*Department of Biochemistry, King's College London, London,* United Kingdom
[3]*BHF Centre of Research Excellence, School of Medicine and Life Sciences, King's College London*
[4]Chemistry Research Laboratory, Mansfield Road, University of Oxford, Oxford OX1 3TA, United Kingdom

Abstract

Molecular dynamics simulations amounting ≈8 μs, demonstrate that the glucose transporter GLUT1 undergoes structural fluctuations mediated by the fluidity of the lipid bilayer and the proximity to glucose. The fluctuations of GLUT1 increase as the glucose concentration is raised. These fluctuations are more pronounced when the lipid bilayer is in the fluid compared to the gel phase. Glucose interactions are confined to the extra-membranous residues when the lipid is in the gel phase but diffuse into the transmembrane regions in the fluid phase. Proximity of glucose to GLUT1 causes asynchronous expansions of key bottlenecks at the internal and external openings of the central pore. This is accomplished only by small conformational changes at single residue level that lower the resistance to glucose movements, thereby permitting un-steered glucose and water movements along the entire length of the pore. When glucose is near salt bridges located at the external and internal openings of the central pore, the distance separating the polar amino acid residues guarding these apertures tends to increase in both, fluid and gel phases. It is evident that the multiplicity of glucose interactions, obtained with high concentrations, amplify the structural fluctuations in GLUT1. The findings that most of the salt bridges and the bottlenecks appear to be operated by glucose proximity suggest that the main triggers to activation of transport are located within the solvent accessible linker regions in the extramembranous zones.

Introduction

The glucose transporter GLUT1 encoded by SCL2A1 and a member of the major facilitator superfamily (MFS), has several well-known properties related to facilitative diffusion of glucose and other hexoses, namely (i) stereo-specificity for transported ligands, (ii) saturability of both ligand binding and transport rates, (iii) competitive inhibition by similar sugars, (iv) different kinetic parameters for net uptake and net efflux defined as asymmetry, (v) capability of inhibition by a multitude of chemicals, some with very high affinity, and (vi) temperature sensitivity.[1, 2] Additionally, there are a large number of mutations with a very widespread distribution over the entire GLUT1 that affect the transport function of the protein causing suboptimal glucose transport that alters its kinetics, temperature sensitivity and asymmetric kinetic properties.[3,4] These mutations give rise to the glucose transporter deficiency syndrome, GLUT1DS.[5] The structural properties of GLUTs have been described extensively using a variety of biochemical and molecular biological techniques,[6] crystallography[7] and computational studies.[8] From these studies, a large body of data indicate that the twelve transmembrane domains of GLUT1 contain at least one centrally located high affinity glucose binding site. However, there is no agreement as to whether this confers stereospecificity or any of the other kinetic properties *e.g.* asymmetry. Recent reviews[9, 10] summarise well the various ways in which the crystal structures of MFS transporters have informed interpretations on how the alternating access model may work. The rocker switch mechanism views the transporter as having two domains, the N and C termini, consisting of the two pairs of six transmembrane domains with linkers holding them together. At the endofacial or inside surface, a long semi-structured linker joins TMs 6 and 7 (Figure 1). Near the mid-point of the central fissure, between these bundle pairs, lies the high affinity binding site, as delineated by crystallography. The bundles are viewed as moving reciprocally in poses that either tilt towards an open outward or open inward posture. Alternation between these two end stage postures is viewed as being the major cause of ligand transit, as it leads to sequential exposure of the binding site to the outside or inside solution. The rocker switch mechanism is-the most favoured for the GLUT1 glucose transport mechanism. An alternative mechanism, where the two domains are structurally dissimilar requires only one mobile domain to rock against the other stable domain. The net effect is similar to that of the rocker switch mechanism in that the central ligand binding domain is alternatively exposed to the outside and inside solutions, such as occurs hypothetically with the Leucine transporte.[11] A third variant of the alternating access model is the ‘elevator mechanism’, where the mobile domain moves mainly in the vertical

plane, instead of the horizontal plane. The elevating bundle alternately raises or lowers the ligand binding site, thereby exposing the ligand to the external or internal solution. Unlike the rocker switch or rocking bundles, this type of transporter consists of 7 +7 TMs and is utilized to transport amino-acids, polyamines and organocations.[12]

Apart from the ligand operated gates preventing ligand leakages through the transporters, and which allow access to the central binding site, all three mechanisms propose that the separate TM bundle domains behave as rigid bodies that move in unison to effect the necessary conformational changes. These conformational changes have been deduced based on X-ray crystallography or 2D EM crystallography of the various transporter substates. Recently several intermediate crystal states between the canonical end stage inward and outward conformations, have been the deduced basis of a detailed trajectory of the elevator-like transitions of the concentrative nucleoside transporter from *Neisseria wadsworthii*.[13] The slow time course of these of conformational changes places them outside the resolution of normal unforced atomistic molecular dynamic (MD) simulations.

Unlike ion or water movements through channels, where throughputs are high and fast, in the nanosecond timescale domain, glucose transport via the specific GLUT1 transporter is relatively slow with turnover rates in the millisecond range *i.e.* 5-6 orders slower than in channels. Simulating this slow process often requires adoption of compromises and shortcuts in the simulation protocols. Many protocols have been specifically designed to corroborate the existing assumptions of the alternating access model of uniport transport; namely, (i) a single high affinity binding site situated around the middle of the central cleft with easy access of ligands from the external and internal solutions, (ii) high resistance to ligand flow across the central binding site which necessitates a major rearrangement of the transmembrane helices into an open inward and open outward poses, and (iii) sometimes, a third occluded intermediate pose. These choices mirror the crystallographic findings[14] and the mainstream assumptions of alternating access transport.[15,16] The most influential of these assumptions is the single centrally located high affinity ligand binding site. A frequent inference derived from it, is that any other ligand binding sites are extraneous to the transport mechanism or selectivity of the kinetics. The low turnover of glucose transport[17,18] rationalizes the assumption that contemporaneous multiple ligand interactions with the transporter must be rare and thus, relatively unimportant. It also justifies the case for steered ligand transits and the Gibbs free energy profiles derived from these, showing the expected high change in Gibbs free energy for forced ligand transit through the central barrier. The central binding site is implied to be a

relatively rigid structured region[19-21] and the transporter must adopt multiple poses necessary to effect glucose transfer.[21-25] Nevertheless, recent MD simulations of glucose passage within GLUT1 have expressed doubts about the need for large scale conformational rearrangements.[24, 26] Chen and Phelix[26] suggested that there are extracellular gates that are dependent on asymmetric lipid distributions and at low temperatures and infinite trans-exchange uptake is dependent on transport of the open chain form of glucose which permits passage through a narrow aperture.

Here, MD simulations have been employed to investigate at atomistic level whether the structural changes and interaction patterns of the bilayer phase contribute to structural modifications in the glucose transporter using GLUT1 embedded in DPPC lipid bilayers under temperature-controlled fluid and gel conditions, in the presence of β-D-glucopyranose and water. The effects of glucose bonding at the surface, its penetration in the protein and its interactions with the protein have been characterised as well as the changes in the dimensions of the central pore and the salt bridge interactions that affect overall the transporter stability, and in turn, have effects on both glucose and water mobility.

The question as to whether large-scale protein conformational changes are necessarily required to achieve glucose transit across GLUT1 remains unresolved to date. Recent papers have demonstrated that glucose transport by GLUTs and other sugar transporters can be accomplished by small-scale perturbations along the entire length of the central pore. These may occur because of both glucose-dependent local induced fits and glucose-dependent allosteric interactions that facilitate global increases in permeability. Our study aims to remove some of the obscurity surrounding these questions by comparing the differences between simulations under flooded conditions with high content of glucose and simulations where glucose is specifically docked within the protein and where the nominal average extracellular glucose concentration is small, in both cases, using relatively long simulation times.

Materials and Methods

System Set-up

The crystal structure of the human glucose transporter GLUT1 (PDB ID: 4PYP), which has a nonyl beta-D-glucopyranoside bound,[27] was used as a starting point for the computational work. The initial systems were generated using the Membrane Builder module of CHARMM-GUI.[28] A membrane patch of 100 Å x 100 Å dimensions was built. The membrane contained 205 molecules of 1, 2-dipalmitoyl-*sn*-glycero-3-phosphocholine (DPPC).

This choice was based on a compromise between size and computational resources. Subsequently, the GLUT1 structure was inserted into the membrane patch. To avoid steric clashes, lipids in close contact with the protein were deleted. This resulted in an asymmetric lipid distribution with 100 lipid molecules in the cytoplasmic leaflet and 105 lipid molecules in the external leaflet. The combined system was solvated with water and ions up to a final concentration of 150 mM NaCl to produce a rectangular simulation box of dimensions 95 x 95 x 105 $Å^3$ and ~100,000 atoms. Several independent simulations were run using different conditions and a summary is displayed in Table 1. Two main protocols were followed. The first one corresponds to 'flooding' simulations where the solution is 'flooded' with substrate and allowed to partition into membrane and protein binding sites over the course of an MD simulation trajectory. An alternative is a structure-based docking protocol followed by MD simulations where the nonyl beta-D-glucopyranoside ligand bound to GLUT1 in PDB 4PYP was replaced by a glucose molecule at this binding site. The MD approach holds several advantages as all protein degrees of freedom are unrestrained, resulting in a fully flexible and dynamic system. In addition, the MD approach naturally includes explicit water and the membrane lipid environment is also included. Furthermore, the MD approach accounts for interactions between glucose molecules, and can therefore identify multiply occupied sites. Two different temperatures were employed, one greater (323.15 K) and one lower (308.15 K) than the gel-to-liquid crystalline phase transition temperature of DPPC 314.15 K.

Molecular Dynamics Simulations

The software NAMD2.13 was employed to perform the MD simulations.[29] The CHARMM36 force field[30] was used to model the protein, glucose and lipids. Standard CHARMM parameters[31] were used for ions, and the TIP3P model for water.[32] Pressure was maintained at 1 atm by a Langevin piston,[33] with a damping time constant of 50 ps and a period of 200 ps. A semi-isotropic pressure coupling method was used in all the simulations. For the NAMD calculations, the pressure of the piston acted independently in each dimension but maintained a constant ratio in the x and y axis, corresponding to the plane of the membrane. The temperature was maintained constant by coupling the system to a Langevin thermostat, with a damping coefficient of 1 ps^{-1}. The particle mesh Ewald (PME) algorithm was used for the evaluation of electrostatic interactions beyond 12 Å, with a PME grid spacing of 1 Å, and NAMD defaults for spline and κ values.[34] A cut-off at 12 Å was applied to non-bonded forces. Both electrostatics and van der Waals forces were smoothly switched off between the switching distance of 10 Å and the cut-off distance of 12 Å, using the default switching function in

NAMD. A Verlet neighbour list with pair-list distance of 13.5 Å was used to evaluate non-bonded neighbouring forces within the pair-list distance.[35] The lengths of covalent bonds involving hydrogen atoms were constrained by the Shake algorithm in order to use a 2-fs time-step.[36, 37] The multi-time step algorithm Verlet-I/r-RESPA[35, 37] was used to integrate the equations of motion. The systems were subject to 10,000 steps of energy minimization, followed by an equilibration consisting of sequential release of various restraints added to the system: (i) harmonic restraints to heavy atoms of the protein and ions, (ii) repulsive restraints to prevent water from entering in the hydrophobic region of the membrane, and (iii) planar restraints to hold the position of the lipid headgroups along the z-axis. Subsequently, production runs were executed at the selected temperatures.

The program HOLE[38] was used to analyze the size and shape of the available pathways for glucose transit from the GLUT1 inward (IN) and outward (OUT) faces to the glucose binding site (GBP) at the center of the protein.

Results & Discussion

The major facilitator superfamily transporters share a conserved core fold that comprises 12 transmembrane segments organized into two discretely folded domains, namely the amino- and carboxy-terminal domains. Within each domain, the six consecutive transmembrane segments are folded into a pair of '3+3' inverted repeats. The structure of full-length human GLUT1 inserted in a model lipid bilayer is shown in Figure 1. The structure of GLUT1 was resolved in an inward-open conformation with a glucose-derivative bound to the main binding site.[7] The D-glucopyranoside of the β-NG molecule found in the crystal structure of GLUT1 is hydrogen-bonded to the surrounding polar residues in the C domain, which provides the primary substrate-binding site as residues from the N domain are not involved in ligand binding. Comparison with ligands found in crystal structures of related proteins suggests the presence of a single sugar-binding site that is alternately accessed from either side of the membrane.[7] The relative motion of the N domain would then result in alternating access.[7] For the purpose of the simulations, the crystallographic sugar-derivative in the crystal was not included in the model or it was replaced by β-D-glucopyranose.

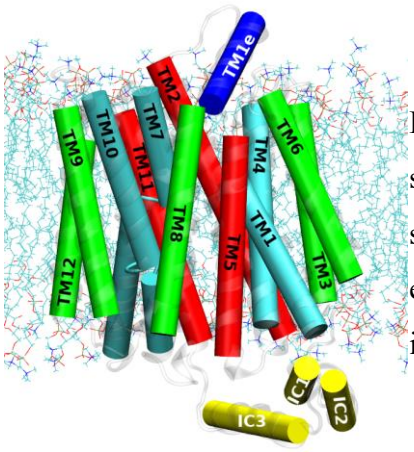

Figure 1. Illustration of the simulation system with the structure of the full-length human GLUT1 in cartoon representation inserted in a model lipid bilayer. Each structural element is labelled; TM stands for transmembrane and IC for intracellular.

Two simulation protocols were followed referred to as 'flooding' and 'docked' simulations, which permit useful comparisons between the effects of both high and effectively zero external glucose concentrations on the mobility of the amino acid residues in GLUT1. To consider how the physical phase of the membrane alters glucose transporter structural dynamics, different temperatures were also adopted, one greater (323.15 K) and one lower (308.15 K) than the gel-to-liquid crystalline phase transition temperature of DPPC which is reported to be 314.15 K. A list of the simulations considered in this study is presented in Table 1.

Table 1. MD simulations considered in this study and some system details. CBS stands for Central Binding Site.

System Notation	Set-up	Temperature (K)	Lipid Phase	Simulation Time [μs]	Glucose at CBS	#Water	#Glucose
Flooded-Fluid (FF)	Flooding	323.15	Fluid	2	NO	20849	48
Flooded-Gel (FG)		308.15	Gel	2			
Docked-Fluid (DF)	Docked	323.15	Fluid	2	YES	21447	1
Docked-Gel (DG)		308.15	Gel	2			

The transient trajectories of glucose entry into and exit from GLUT1 were analysed and are shown in Figure 2 and Supplementary Material Figure S1. It should be noted that the movements of both glucose and water within the entire trajectory are diffusive as no steering forces were applied; the only forces acting on the ligands are those generated by the fields of the protein amino acids, membrane lipids and the ions in the solution. In the flooded-fluid simulations, glucose penetrates and crosses the midline several times, whereas glucose does not penetrate beyond the superficial regions of GLUT1 under the flooded-gel condition during the period of the simulations. In both, gel and fluid-docked conditions (Figure S1, Supplementary Material), the single docked glucose ligand escapes to the external solution within 250 ns of initiation the trajectory but makes frequent and short-lived returns to the superficial

layers of the transporter, throughout the remaining trajectory. The most notable feature within the flooded-fluid trajectory is that a glucose ligand crosses and retraces its steps back across the midline through a 'high affinity' central site of the main pore several times during the microsecond and it remains within the transmembrane domain (Figure 2.B). This is the first instance of un-steered spontaneous transits of glucose across the central 'high affinity' binding site. Given the available computational resources, we opted to run long equilibrium simulations rather than several shorter replicas. The fact that only a single translocation of a glucose molecule through the central pore of the protein was observed is not surprising considering there is not a concentration gradient of glucose due to the periodic boundary conditions. In effect, this observation is a rare event and if we wanted to study translocation *per se,* enhanced sampling techniques (such as metadynamics or the adaptive biasing force method) would be required instead of equilibrium MD simulations.

Although there is evidence from the simulations of tunnel branching at the internal and external surfaces, only one main central channel is apparent for glucose transit. We use the word 'main' to distinguish the central pore from any subsidiary channels that might be as during the simulation, there are at least two portals to glucose and water in the external surface and probably three or more in the internal. Glucose remains for a significant dwell time in the central zone of the main pore where it oscillates and fluctuates between H-bonding sites at G384-T137 and V165-P385 for three periods between 1050-1190, 1210-1290 and 1450-1570 ns. These prolonged dwell times within the central pore could be considered as binding events. However, examination of the H-bonding behaviour of glucose shows that it does not remain fixed at any site for more than a few nanoseconds, instead, it moves along with water within the confines of the central cavity. In addition to the single glucose molecule that translocates through the pore of GLUT1 as shown in Figure 2.A, several other glucose molecules are also present within the internal and external margins of the GLUT1's transmembrane region for periods longer than 40 ns (Figure 2.B and 2C, Figure S1). Glucose at the external surface of the protein makes frequent, but transient H-bonds with the protein residues exposed to the solution.

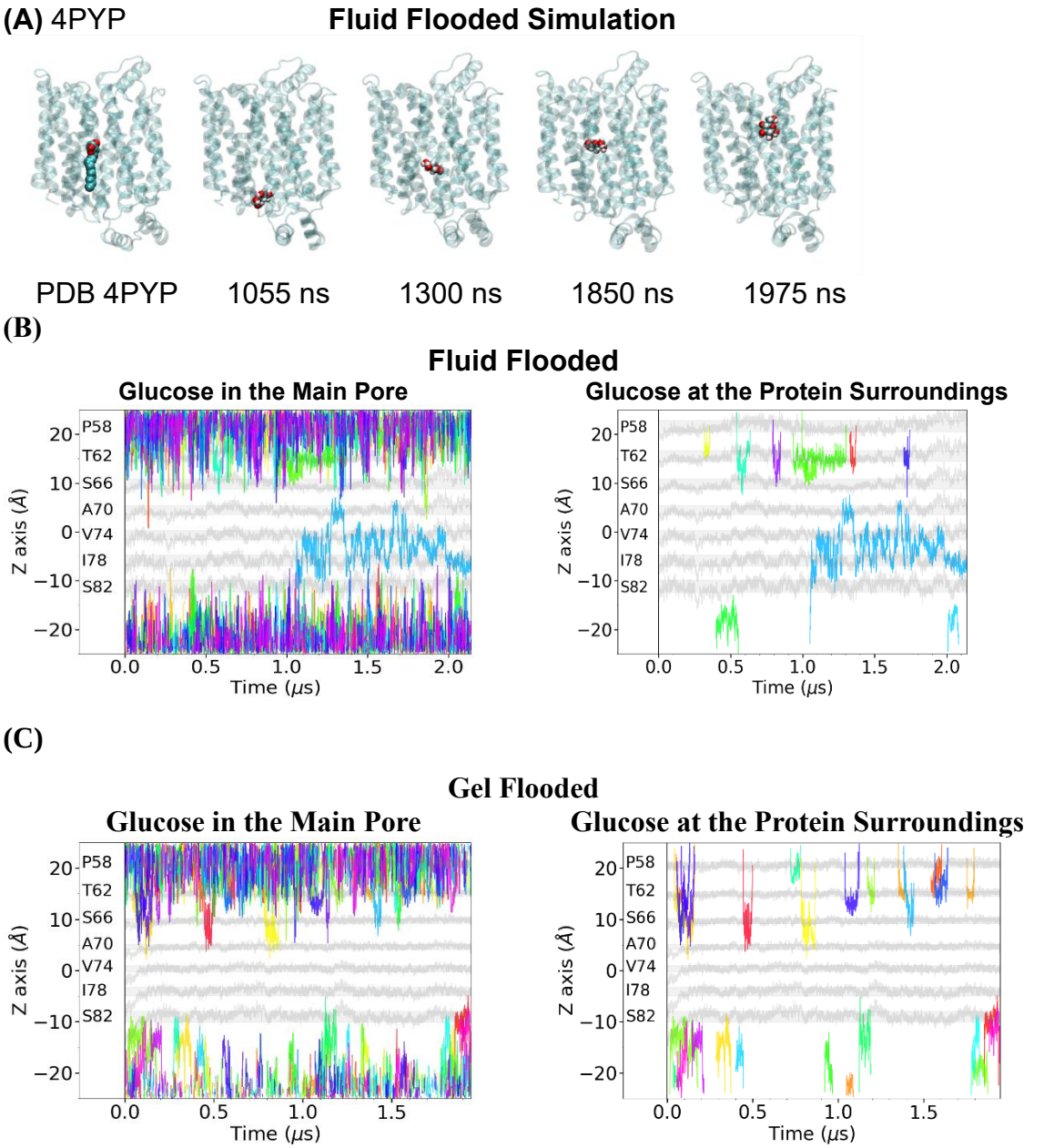

Figure 2 (A) Pathway that a glucose molecule follows through the protein pore referenced to the crystal structure in PDB id 4PYP that has nonyl beta-D-glucopyranoside from the fluid flooded trajectory. **(B)** Glucose forms multiple transient hydrogen bonds with extramembrane domains of GLUT1. Evolution of the positions of the centre of mass of different glucose molecules either along the main pore of the protein or outside the protein in the surrounding medium in the flooding simulations. Only glucose molecules that remain either in the pore or bonded with extramembranous residues for a period of over 40 ns are shown using different colours. The origin of the z-axis corresponds to the centre of mass of the lipid membrane.

The backbone atom root-mean-square deviation (RMSD) values were computed for the trajectories taking as a reference the initial x-ray structure. The convergence to a specific value within the resolution of the initial x-ray structure (3.17 Å) suggests that the protein structures remained relatively stable. Overall, the RMSD values of GLUT1 in the fluid membrane condition are greater than in the gel membrane condition; the RMSD of GLUT1 averages ≈ 1.9Å

and ≈ 1.3 Å in the fluid and gel flooded simulations respectively. Furthermore, there are no significant effects of glucose on the RMSD during the instances when glucose traverses the central regions in the time interval between 1.0 and 1.5 μs in the fluid flooded trajectory. The major effect of glucose is on the root-mean-square fluctuation (RMSF) values of the extramembranous regions, as has been previously reported.[26] When comparing the effects of the presence or absence of glucose in the RMSF of the protein in the fluid flooded system (Figure 3.A), it can be observed that glucose interactions increase the magnitude of the RMSF values in the fluid membranes in the region of the external linkers between transmembrane helices by approximately 0.75 Å. The magnitude of the glucose-dependent increases in the three C-terminal external linkers are around twice those seen in the three N -terminal external linkers. In the case of internal linkers, only the structured elements in the large linker between TMs 6-7 and the links between TMs 8-9 and TMs 10-11 show glucose-dependent changes. Additionally, there are regions where glucose decreases the RMSFs *e.g.* the external part of TM1 and TM3, the external linker between TMs 5-6, and in the unstructured region of the large linker (residues 230-235). However, these glucose-dependent increases extend from the exposed extramembranous regions into the TMs, particularly those in the N-terminal half.

Glucose modulation of the dynamics of extra-membranous domains of GLUT1 depend on membrane fluidity. The effects of fluid-gel transformation of the membrane lipid on the external glucose dependent RMSFs are shown by comparison of the red versus green traces (Figure 3.B). Apart from residues L109-F112 at the outer regions of TM3, gelling leads to a sharp decrease in the RMSF values. These decreases are most profound in the more mobile extra membranous regions but also extend into the TM regions, particularly of TM 1,2,4,6, the outer part of TM7 and TMs 9-12. When examining the fluid flooded RMSFs in various time intervals during the trajectory (Figure 3C, 3D), correlations can be observed between the RMSFs in the external linker regions between TM1-2 and 7-8, and TM9-10 at the external surface, and the linker between TM4-5 and 6-7 and TM8-9 and 10-11 at the endofacial surface *e.g.* the intracellular side of the membrane. In contrast, the time dependent RMSF changes related to the positions of glucose in the flooded-gel condition mainly occur at the external linkers.

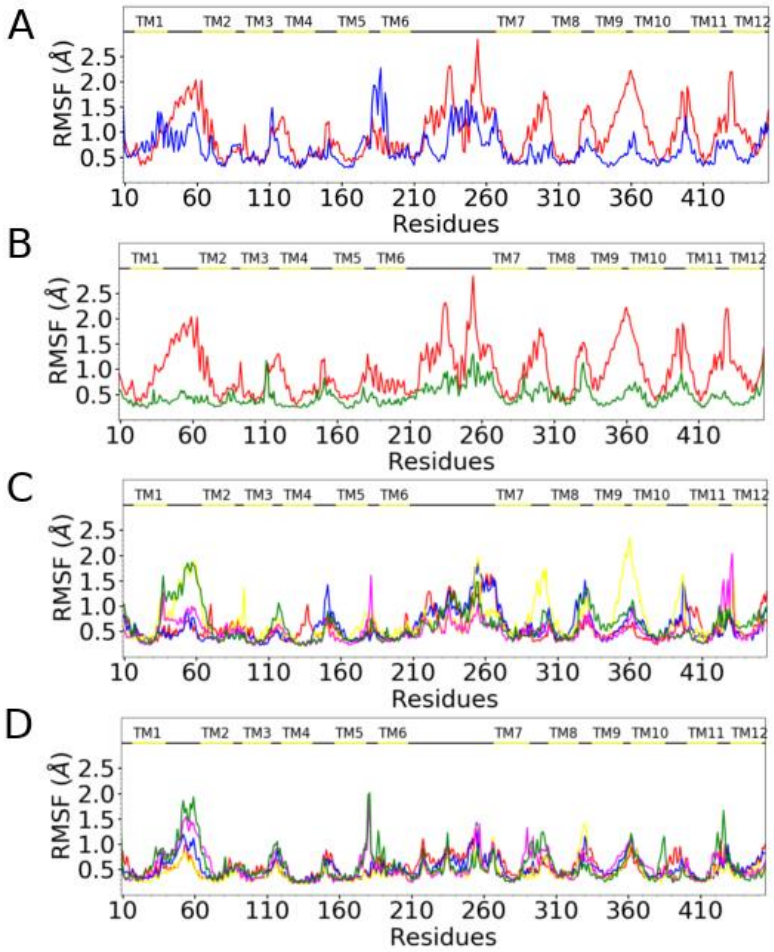

Figure 3. Comparison between the Cα RMSFs of the protein in different trajectories: (A) fluid flooded trajectories in the presence (red) or absence (blue) of glucose in the pore, (B) fluid (red) versus gel (green) flooded systems, and fluid flooded simulation divided in several time intervals of 0.2 μs from: (C) 0 to 1 μs (0-0.2 red, 0.2-0.4 blue, 0.4-0.6 yellow, 0.6-0.8 magenta, 0.8-1.0 green) and from (D) 1 to 2 μs (1.0-1.2 red, 1.2-1.4 blue, 1.4-1.6 yellow, 1.6-1.8 magenta, 1.8-2.0 green).

The relative frequency of glucose interactions with GLUT1 residues was characterized by calculating the H-bond interactions between glucose and residues of the protein along the central pore axis as a function of time (Figure 4). In the docked simulations, the frequency of glucose interactions is negligible. Unsurprisingly, the most frequently encountered residues by glucose are those in the extramembranous regions, particularly around residue Val290 in TM7 and the external linker between TM7-8 and the internal linker between TM6-7. In the gel state, the frequency of these interactions is greatly reduced in the intramembranous TM regions.

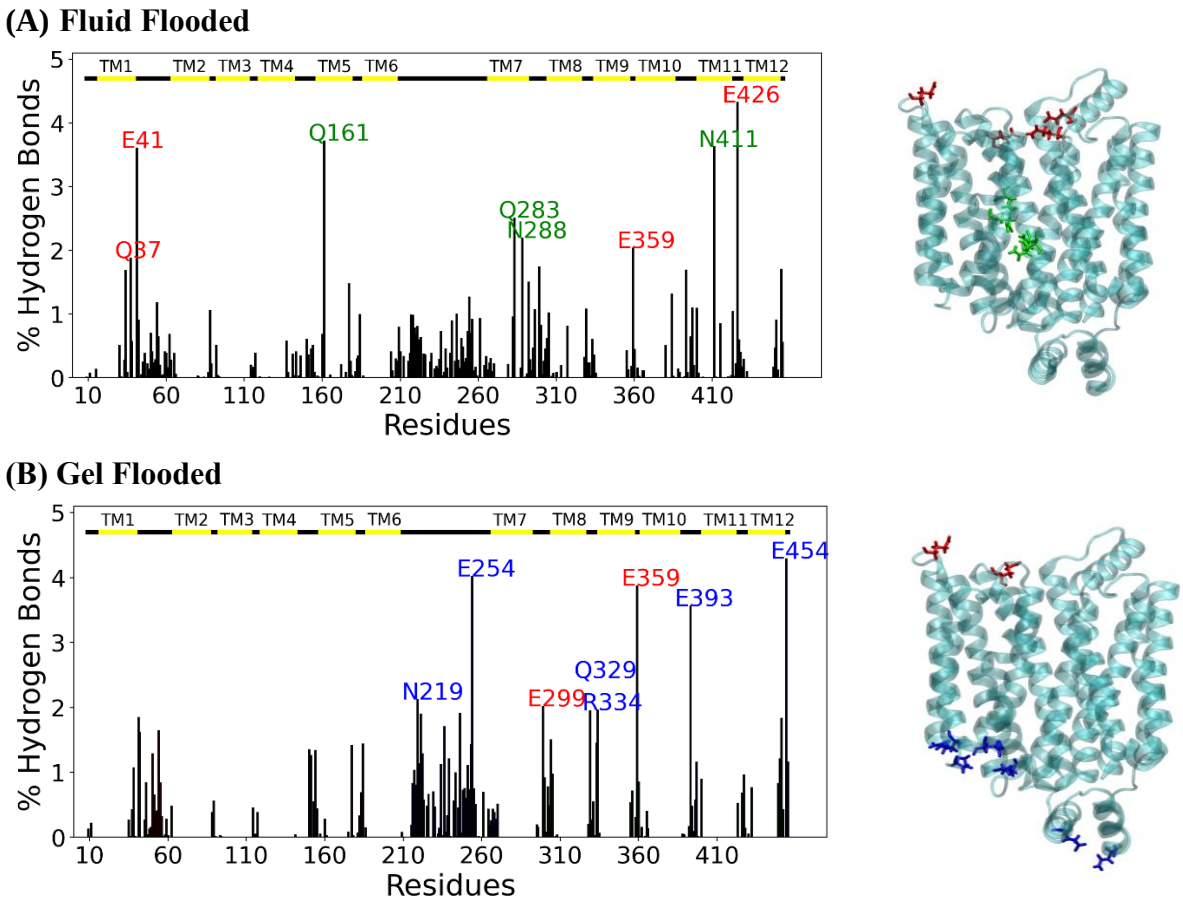

Figure 4. Most frequent extramembranous glucose hydrogen bonds are observed in external linkers between TM6-7 and TM7-8. Percentage of hydrogen bonds referenced to the total number of hydrogen bonds accounted during the whole trajectory shown for the (A) fluid and (B) gel flooded simulations. The eight residues that established the highest number of H-bonds are labelled. From each simulation, a snapshot of the protein in new cartoon representation is presented with the residues highlighted in the plots shown in licorice representation and coloured according to their position: red (extracellular side), blue (intracellular side) and green (central position).

The degree of mobility of every amino acid residue was monitored and the influence of glucose on this parameter was mapped for both the flooded and docked conditions as shown in Figure 5. This measure monitors dynamical changes in residue movements. The residues in contact with glucose during its progress through the central pore regions move more in the time interval between 1.5 - 2.0 μs in the fluid flooded simulations in comparison with the fluid docked. The fluid flooded map shows that the outer half of TM1 is unsettled from 1.7 to 2.2 μs, as are the outer parts of TM9-10 and TM11-12. Almost all the glucose-dependent increase in residue movements is confined to the extramembranous regions in the fluid flooded trajectory. There is significantly less change in residues within the intramembranous regions.

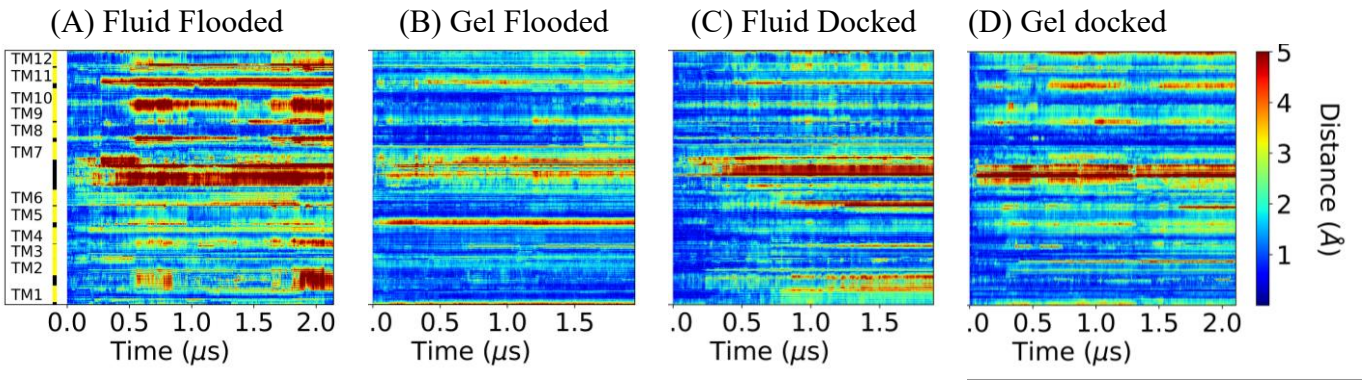

Figure 5. Glucose hydrogen bonding amplifies extramembranous motion of TM linker segments of GLUT1. Evolution of the displacement of the protein Cα atoms during the trajectory referenced to the starting structure as a function of the structural elements in (A) fluid and (B) gel flooded simulations, and (C) fluid and (D) gel docked.

Glucose also displaces water in the central pore. We had shown previously that water is displaced from the cavities of GLUT1 when the bilayer undergoes fluid to gel phase transition.[39] In the present simulations, it is evident that glucose displaces water from the margin towards the central zone of the pore of GLUT1 in fluid bilayers as well as from marginal zones in the gel bilayers (Figure S2). Water densities and water displacement by glucose are reflected in changes of the dimensions of the central pore of GLUT1. At low glucose concentration, in the fluid docked condition, reductions are observed in the width and dimensions of the pore at both internal and external margins of the transporter. In the fluid flooding simulations, during the time from t = 1.1 to 1.7 μs, the presence of glucose in the central region changes the channel shape by decreasing its length by 6 - 7 Å and widening its diameter by a similar distance, thereby changing the cavity from an oblate to a more spherical structure.

When glucose penetrates the intramembranous regions of GLUT1 at t = 1.1 μs, the ratio of water: glucose H-bonds decreases from around 0.9 at Z = -20 Å to ≈ 0.5 as glucose penetrates to Z = +6.0 Å. It is apparent that the more deeply glucose penetrates the transmembrane region, the more water it tends to displace until it reaches the hydrophobic regions of the pore between 6 - 12 Å (Figure 6).

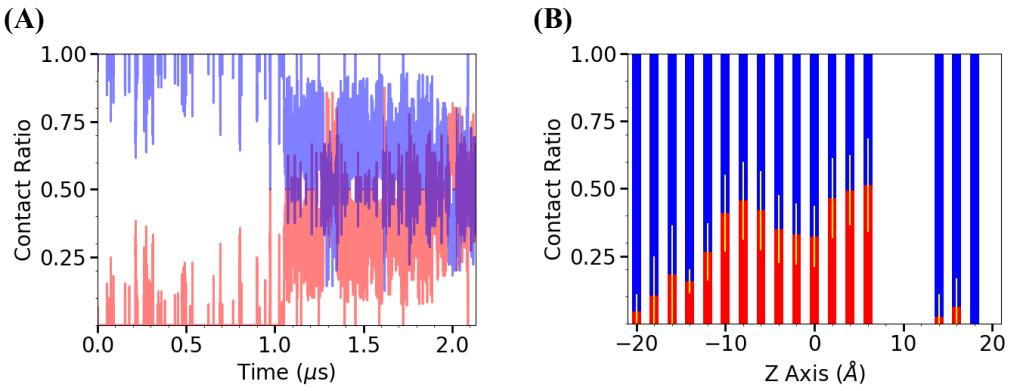

Figure 6. Evolution of the protein central pore along the Z axis in the fluid-flooded simulation. (A) Ratio of glucose (red) and water (blue) around the protein atoms. The distance between two atoms is considered a contact when <4.5 Å. (B) The ratio is averaged along the pore axis with a bin width of 2 Å.

Glucose exerts both direct and allosteric effects to modulate the width of the GLUT1 pore. The pore radius of GLUT1 has been mapped along the axis perpendicular to the membrane plane at different times during the trajectory of the flooded simulation in the fluid state (Figure 7). Three bottlenecks in the central pore have been previously identified as barriers to glucose movement. The widths of these bottlenecks are variable, as was shown previously.[39] Amongst other factors the barrier widths are controlled by membrane fluidity. However, membrane fluidity as regulated by temperature, is generally fairly constant in mammals, so in isothermal conditions, the direct influence of transported ligands on the flexibility of the protein is likely to be more important in determining the mobility of a transported ligand through bottlenecks.[40] Concepts of protein flexibility and rigidity have been associated with static mechanical or crystallographically determined structures that are not always entirely relevant to protein fluctuations when embedded in a fluid environment. Thus, bottlenecks imposed by adjacency of large aromatic sidechains or salt bridges can be altered by interposing shielding ligands*, e.g.* glucose or water. A bottleneck blocking glucose uptake at the extracellular surface has been observed in both GLUT1 and GLUT3, and XylE.[14, 24, 26, 39] Another was reported[25, 41] in the central cavity of GLUT1 due to movements of sidechains Gln282 and Tyr292. It has been proposed that the central cavity is obstructed by Tyr291 Tyr292 and Asn288 whereby an axial rotation results in an outward open to outward occluded conformations.[7] However, in an earlier docking study involving a relatively short (10 ns) simulation, no high affinity site within the central cavity was observed. Instead, it was found that glucose captured within the cavity, diffused randomly between several H-bonding sites.[42] The current study corroborates this view; another bottleneck was observed at Phe389, Trp388, Arg400 and H160 at the endofacial end of the central pore.[22, 26, 39]

(A) **(B)**

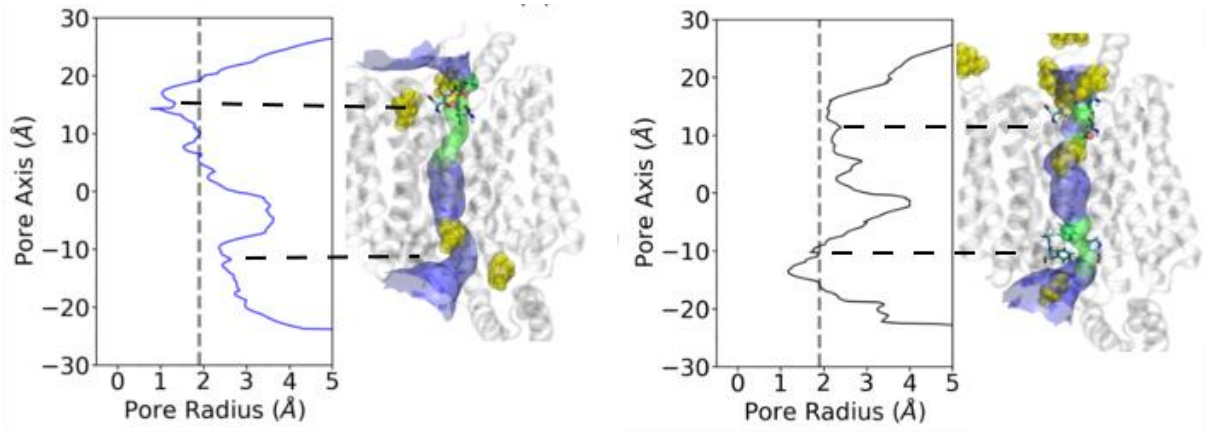

Figure 7. The presence of glucose alters pore dimensions and dynamics. Pore profiles of the protein and radius of the central path along the pore axis in the fluid flooded system is shown for two representative snapshots at (A) time = 1.05 μs when the pore is open towards the external side, and (B) time = 1.3 μs when the pore is open towards the intracellular side. The dotted vertical line indicates the minimal pore radius through which D-glucose would get through.[43] Next to the pore radius profiles, a representative snapshot illustrates the 3D central tunnel using the following colour code: red represents the volume where not even water molecules are able to pass, green represents the volume where small molecules like water can get through, and blue is the volume large enough where bigger molecules can cross. The horizontal dotted lines linking the graphs and the 3D hole profiles correspond to the bottlenecks of the pore. Residues that delimit the bottleneck are represented in licorice. The protein is shown in new cartoon representation in grey and glucose molecules in yellow are depicted in vdw representation.

In the fluid flooded trajectory, two major bottlenecks are observed at either ends of the pore, an external one at Z = 16 - 20 Å and an internal one at Z= -15 to -10 Å**.** However, these constrictions are not permanent features and there is considerable variability in the width of both the external and internal bottlenecks. These changes are asynchronous**.** At t = 1.055 μs, the external barrier has a radius of ≈ 1.0 Å and the internal barrier a radius of 2.3 Å, whereas at t = 1.300 μs, the internal barrier has a radius of 1.2 Å and the width of the external barrier is increased to 2.2 Å. When the external barrier is open, two glucose molecules are H-bonded to adjacent residues, Thr295 and Gln37, both of which are directly accessible to the external solution. When the internal pore opening is at its widest diameter, two glucose molecules are adjacent H-bonded to Phe291and Pro141. The requirement for glucose proximity to enable glucose access through the barrier is ratified by the observation that in the fluid docked trajectory, where glucose is initially absent from the external solutions, the pore radii never exceed the minimum 1.9 Å required for glucose passage**.**

Glucose modifies salt bridge networks of extramembranous domains of GLUT1. The effects of glucose on GLUT1 dynamics thus far have been considered mainly at a global level. However, the underlying effects of glucose actions are due to interactions at atomic levels. Several sets of salt bridges have been observed between either Glu or Asp and either Lys or Arg, at

both ends of the central pore.[26] In several cases, the bridged pairs are in close enough proximity to switch between pairings. We find that the proximity of glucose perturbs these networks, notably between Arg400 and Glu393, and Glu247, Arg153 and Glu393. Glucose binding to this network tends to open gates and permit water infiltration into the central channel (Figure 8). Once glucose penetrates, partial closure of the gate can form a semipermeable barrier which generates a local intramolecular osmotic flow of water,[44, 45] as is observed in the flooded simulations in both fluid and gel conditions. In fluid bilayers with 1 mM glucose, prolonged opening of the gates at the external and internal ends of the pore leads to the entire central pore filling with large numbers of water molecules (≈ 30 - 40). During prolonged gate closure water drains from the central pore. These findings indicate that water does not remain static within the central pore and that the hydrophobic sidechains lining the channel are permissive to water movement.

The effects of glucose proximity on the bottleneck widths in GLUT1 are similar to those previously observed in acetylcholinesterase, where allosteric ligand opens the bottleneck widths within the 'gorge' that normally prevents access substrate access to the active site at 20Å depth from the solution interface. In this system too, complex multiple allosteric ligand interactions are showed by MD to increase the catalytic functionality of enzyme by causing small fluctuations in the protein that permit the bottleneck to open sufficiently to provide access to sites which crystallography deems to be unreachable.[46]

(A)

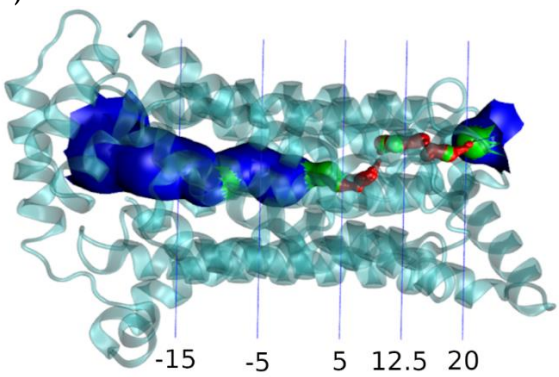

(B)

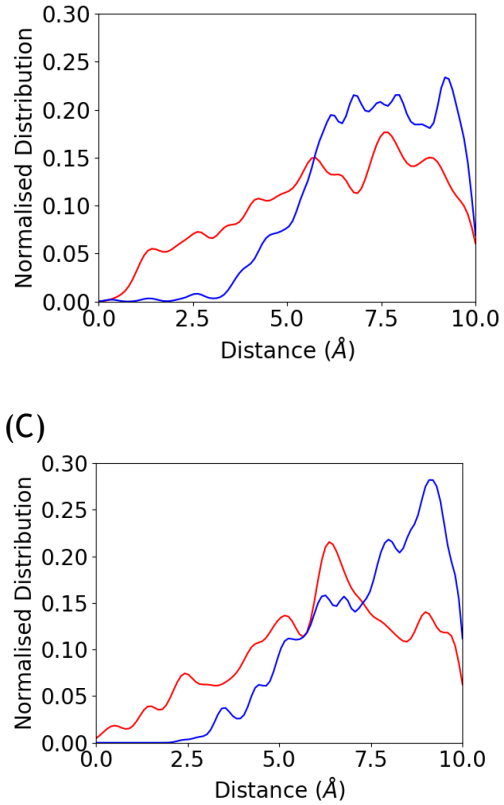

Figure 8. Relationship between the bottleneck radius and the proximity of the nearest glucose molecule in two sets of positions along the Z-axis of the transporter corresponding to the intracellular (-5.0 to +5.0 Å) and extracellular (12.5 to 20.0 Å) directions from the center as indicated in (A). (A) Crystallographic structure in new ribbons representation colored in cyan and its pore profile in red where the pore radius is too tight for a water molecule, in green where there is room for a single water and in blue where the radius is at least double the minimum for a single water molecule. Effects of glucose proximity on the distribution of the external (red) and the internal (blue) bottleneck for the (B) flooded fluid and (C) flooded gel systems. The minimal radius of a glucose molecule was considered to be 1.9 Å.[39]

The effect of glucose proximity on the distance separating polar residues forming salt bridges was analysed (Supplementary Material Figure S3, S4). A systemic examination of all the salt bridges between Glu or Asp and Lys or Arg yields 17 salt bridges in the flooded simulation in the fluid bilayer and 20 salt bridges in the gel condition. Some of these pairs are between single acidic residues and two alternate basic residues *e.g.* Glu236-Lys225 and Glu236-Lys229 or Glu299- Lys300 and Glu299 and Lys38. It is apparent that the distances separating the polar side chains of some salt bridges at the external and cytosolic faces of GLUT1 increase according to the relative proximity of glucose permitting passage of water and glucose into the intramembranous regions of the transporter.

These simulations of GLUT1 in fluid and gel phase bilayers demonstrate unforced glucose transits throughout the length of the central pore of the protein. Glucose facilitates its own passage through the central pore by interacting with the transporter, both globally and at local

levels, thereby generating wider pore openings. Several glucose transits through the central bottleneck are observed during 2 μs in the flooding simulations in fluid bilayers. It has been claimed that asymmetric bilayers with physiological distributions of lipids are necessary to facilitate glucose diffusion via GLUT1 without large scale conformations motions.[47] Although physiological distribution of lipids within the bilayer may improve transport, here, a standard fluid symmetrical DPPC bilayer permitted un-steered glucose diffusion along the entire length of the central pore. Similarly, simulations of the SWEET plant glucose transporters in a symmetrical lipid bilayer gave satisfactory un-steered glucose transport rates.[48, 49] An explanation for the glucose transits observed in the present investigation is that the protocol generates multiple contemporaneous glucose-protein H-bond interactions at both internal and external transporter surfaces. In the absence of a significant glucose concentration in the external solutions, as in the fluid docked protocol, glucose molecules remain confined to the peripheral extramembranous regions of the transporter. When GLUT1 embedded in fluid membranes is exposed to glucose in the flooding simulations, the RMSD and RMSF values of the extramembranous regions and several TMs, in particular TMs 7-12, are greatly increased. These increases result from the multiple H-bond interactions of glucose with the majority of exposed extramembranous residues and with the external portions of TM1, TM2 and TMs 9–12. The increased mobility of the majority of extramembrane residues, combined with the more localised direct and indirect actions of glucose on intramembranous protein as it permeates the central pore, leads to transient widening of the bottleneck regions, which in turn permits greater glucose mobility than hitherto reported in previously published MD simulations.[50, 51]

When GLUT1 is embedded in membranes in the gel phase under flooding conditions, glucose still leads to H-bonding with the exposed residues, although with a much-reduced frequency reflected in the reduced RMSD and RMSF values due to the greater restraint on both protein and membrane movement imposed by the increased lipid viscosity.[52, 53] Perturbations are no longer transmitted into the intramembranous zones as the allosteric propagation is curtailed. Hence, glucose is prevented from deep penetration into the transporter.

It can be observed from our MD simulations that flooding with glucose ‘activates’ GLUT1 and increases its permeability to both glucose and water, and possibly other ligands that can penetrate the GLUT1 porous labyrinth. This view is confirmed by the demonstration that flooding with glucose increases the probability of wider separations occurring in 12/17 salt bridges in the fluid flooded condition and in 11/20 salt bridges in the gel flooded state.

An obvious question is whether there is any experimental evidence to corroborate these in-silico findings. Although it has been largely dismissed as an epiphenomenon, water flows through glucose transporters in erythrocyte membranes were observed in the 1970s.[54, 55] Low concentrations of phloretin (250 μM) reduced both glucose and water permeabilities. Oocytes expressing GLUT1 have a water permeability in the order of $0.28 – 1.7\times10^6$ molecules s^{-1} that is suppressed by 20 μM phloretin.[56] The GLUT1 water permeability is increased by 20 % by exposure to glucose (5 mM). However, increasing glucose concentration to 10 mM reduced the water permeability by approximately 40%.[56] This biphasic effect of glucose on water permeability is also seen with maltose and L-glucose, suggesting that the inhibition of water permeability may be affected by non-penetrating ligand binding to external groups.[57]

GLUTs are also permeable to arsenicals, $As(OH)_3$ and $CH_3As(OH)_2$, possibly via water pathways. However, GLUT1 inhibitors, Hg(II), cytochalasin B and forskolin reduced uptake of glucose but not of $CH_3As(OH)_2$. These results indicate that $CH_3As(OH)_2$ and probably water partially share a common translocation pathway in GLUT1 with parallel branches for glucose transport and water[58] and are supportive of the view that there are multiple branched pathways within GLUTs, some of which are too narrow to permit glucose flows. Similar deductions about multiple entry ports at the exofacial surface had been derived using maltose as a partial inhibitor of glucose uptake[59, 60] and with various GLUT1 mutants which partially blocked glucose uptake *e.g.* T295M.[61, 62]

Maltose, is a non-transported disaccharide with affinity for the external side of the glucose transporter.[63] At concentrations > 1.0 mM, maltose inhibits 3-O-methyl glucose (3OMG) transport ($K_i \approx 12$ mM).[60] However, at concentrations in the range 0 - 1.0 mM, maltose and maltotriose increase the rate of 3OMG transport by ≈ 40%. L-sorbose has a similar low affinity to L-fructose for GLUT1.[64] An anomaly with sorbose transport is that its inhibition by equilibrium glucose concentrations is much greater than predicted by alternating carrier $K_i = \approx 20$ mM.[65, 66] Low glucose concentrations reduce the Arrhenius activation energy E_a of sorbose net exit from 63.9 ± 13 kJ mol^{-1} in glucose-free solution to 42 ± 5 kJ mol^{-1}, when glucose was present in the range 5-10 mM.[44, 67] Thus, glucose, whilst competing with sorbose binding sites, also increases its permeability by decreasing the energy barrier for its transport. This explains why the apparent affinity of glucose-dependent inhibition of sorbose flux decreases. These findings are now explicable by the hypothesis that multiple contemporaneous glucose H-bonding interactions lead to global agitation of GLUT1 which tends to open

bottlenecks within the protein and leads both to a generalized increase in permeability and a specific increase in glucose transport.

Conclusions

GLUT1 is one of the 13 members of the human glucose transport protein family and a membrane-spanning protein that mediates glucose transport into the brain. GLUT1 is necessary for the maintenance of proper glucose delivery to brain via brain capillary networks, blood flow and blood-brain barrier integrity, as well as glial function and structure. Thus, it is crucial to understand at the molecular level the mechanisms of glucose transport.[68, 69] Several putative mechanisms for protein-mediated transport have been proposed. Among the models are two competing hypotheses that have been presented. The first is the simple alternating access mechanism that sequentially presents mutually exclusive exofacial and endofacial substrate-binding sites. The second is the fixed-site transporter with co-existent exofacial and endofacial sugar-binding sites.

This study has shown the importance of ligand operated gating mechanisms at the bottleneck which guard the opening orifices of the central channel and within the network of external water channels in the extramembranous linker regions of the protein. The role of flooding, that initially activates the solution exposed residues that surround the external vestibule and the structured elements of the endofacial linkers, and in the fluid flooded condition is transmitted along the length of the central channel, has shed some light into the molecular basis of glucose transport in GLUT1.

It is apparent that GLUT1 presents multiple substrate and ligand interaction sites. High frequency of ligand interactions with these sites increases the root-mean-squared fluctuations of the exposed residues and this agitation prises open the portals to the wider central region of the channel. Our simulations show that glucose remains trapped within the confines of doubly gated central region where it is relatively free to diffuse as previously observed.[41] These findings are inconsistent with the orthodox view based on a high affinity central binding site based mainly on crystallography of the static GLUT1 structure,[8, 70] in which glucose is bound in relatively immobile complex that requires a large conformational change to allow it to cross this central high affinity binding region.

On the contrary, we observe that the centrally located glucose ligand is relatively mobile and its access to the external solution is mainly controlled by the ligand operated bottlenecks and salt bridges at either end of the pore, consistent with the gating processes at either side of the channel being the main controllers of ligand transit. This shift in emphasis of the control of

transit frequency from a mobile single centrally located binding site to a widely distributed network of sites located in the extramembranous zones of the transporter, may also shift the focal point of search for the ligand stereospecificity sites from the central regions of the transporter where ligand access is seen to be generally hindered, to the much more accessible residues at the exposed surfaces of the transporter as shown by maps of the glucose-H-bonding sites.

This paper illustrates that inferences relating to GLUT1's transport mechanism made solely based on static crystallographic postures may only give a partial mechanistic view. The findings here indicate that multiple glucose interactions at the external and internal surfaces lead to increased access of the central intramembranous zone to water and glucose permeation. Furthermore, we have confirmed that the commonly supposed central 'high affinity' site is not a binding site, but a cavity with bottlenecks at both ends that leads to transitory caging of entrapped ligands until they encounter an escape route. This implies that the ligand throughput through the transporter depends on openings and closures at the external and internal sides of the channel. These apertures at the external surfaces are partially dependent on glucose proximity, suggesting that the sites of the transporter for ligand specificity recognition are situated within the extra membranous portions of the transporter, rather that exclusively in the central zones, as the alternating access view suggests.[71]

Our study corroborates the findings of a recent extensive search for novel inhibitors of GLUT showing three regions of interest for ligand binding in GLUT1. The traditional central zone, where ligands bind with very high affinity and two other zones with direct access to the external and internal bathing solutions, where multiple inhibitor ligands bind with lower affinity.[72] Our findings might suggest that it may be these lower affinity sites the major determinants of ligand specificity.

AUTHOR INFORMATION

Corresponding Authors

Carmen Domene, Email: mcdn20@bath.ac.uk
Richard Naftalin, Email: richard.naftalin@kcl.ac.uk

Author Contributions

The manuscript was written through contributions of all authors. R.N. and C.D. designed the research; S.G-R. and C.D. performed the research; S.G-R. and R.N. analyzed the data. R.N. and C.D. wrote the paper. All authors have given approval to the final version of the manuscript.

ACKNOWLEDGEMENTS

We acknowledge PRACE for awarding access to computational resources in CSCS, the Swiss National Supercomputing Service, in the 17th Project Access Call.

SUPPORTING INFORMATION

Table S1. Effects of glucose on the distances between the polar residues involved in salt bridges in GLUT1. **Figure S1.** Evolution of the position of the centre of mass of the glucose molecule either along the main pore of the protein or outside the protein in the docking simulations. **Figure S2.** Glucose displaces water when hydrogen bonded to GLUT1 and expands the transit pore dimensions. **Figure S3**. Most frequent extramembranous glucose hydrogen bonds are observed in external linkers between TM6-7 and TM7-8. **Figure S4.** Examples of four sets of salt bridges that are proximity regulated in the fluid flooded condition.

This information is available free of charge via the Internet at http://pubs.acs.org.

DATA and SOFTWARE AVAILABILITY

- Requirements for **existing software** applies to this manuscript:

Specific open access software from third parties was used:
NAMD2.13 (https://www.ks.uiuc.edu/Research/namd/2.13/features.html)
VMD1.9 (http://www.ks.uiuc.edu/Research/vmd/)
HOLE (http://www.holeprogram.org/)

- Requirements for **data sharing** applies to this manuscript:

Parameter files are publicly available from: http://mackerell.umaryland.edu/charmm_ff.shtml
Molecular structures used are available from: https://www.rcsb.org/
Input files were generated with CHARMM-GUI (http://www.charmm-gui.org/)
Output files are available from the corresponding author upon request.

Table of Contents (TOC)/Abstract Graphic

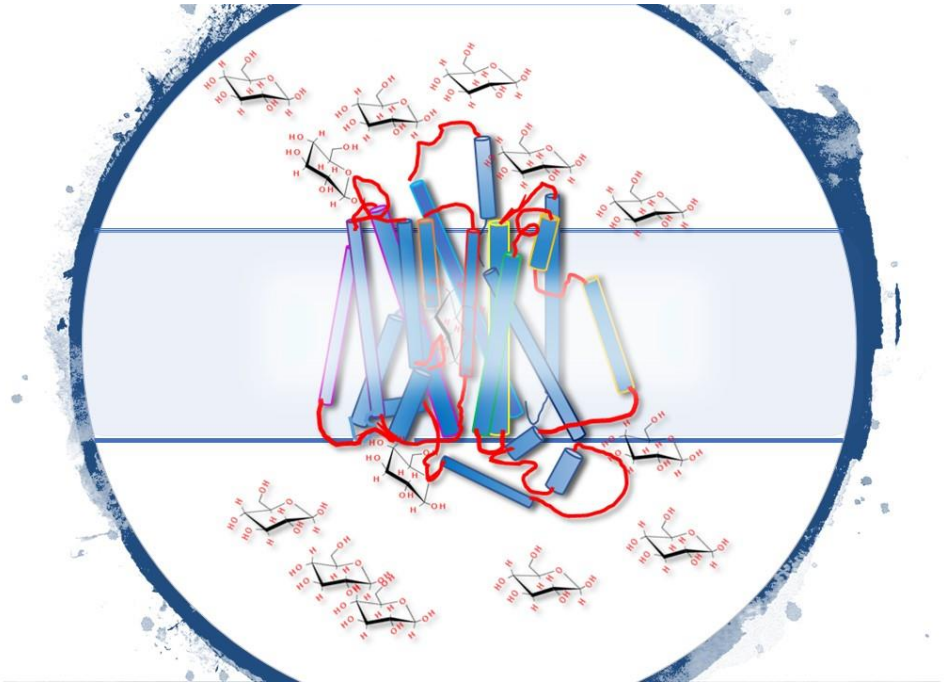

References

1. Carruthers, A.; DeZutter, J.; Ganguly, A.; Devaskar, S. U., Will the original glucose transporter isoform please stand up! Am.J. Physiol. Endocrinol. Metab **2009,** *297*, E836-48.
2. Holman, G. D., Structure, function and regulation of mammalian glucose transporters of the SLC2 family. *Pflügers Archiv - Eur J of Physiol* **2020,** *472*, 1155-1175.
3. Fujii, T.; Ho, Y. Y.; Wang, D.; De Vivo, D. C.; Miyajima, T.; Wong, H. Y.; Tsang, P. T.; Shirasaka, Y.; Kudo, T.; Ito, M., Three Japanese patients with glucose transporter type 1 deficiency syndrome. *Brain Dev* **2007,** *29*, 92-7.
4. Nakamura, S.; Osaka, H.; Muramatsu, S.; Aoki, S.; Jimbo, E. F.; Yamagata, T., Mutational and functional analysis of Glucose transporter I deficiency syndrome. *Mol Genet Metab* **2015,** *116*, 157-162.
5. Rotstein, M.; Engelstad, K.; Yang, H.; Wang, D.; Levy, B.; Chung, W. K.; De Vivo, D. C., Glut1 deficiency: inheritance pattern determined by haploinsufficiency. *Ann Neurol* **2010,** *68*, 955-958.
6. Hollmann, M.; Maron, C.; Heinemann, S., N-Glycosylation site tagging suggests a three transmembrane domain topology for the glutamate receptor GluR1. *Neuron* **1994,** *13*, 1331-1343.
7. Deng, D.; Xu, C.; Sun, P. C.; Wu, J. P.; Yan, C. Y.; Hu, M. X.; Yan, N., Crystal structure of the human glucose transporter GLUT1. *Nature* **2014,** *510*, 121.
8. Deng, D.; Yan, N., GLUT, SGLT, and SWEET: Structural and mechanistic investigations of the glucose transporters. *Protein Sci.* **2016,** *25*, 546-58.
9. Drew, D.; North, R. A.; Nagarathinam, K.; Tanabe, M., Structures and general transport mechanisms by the major facilitator superfamily. *Chem Rev* **2021,** *121*, 5289-5335.
10. Diallinas, G., Transporter specificity: a tale of loosened elevator-sliding. *Trends in biochemical sciences* **2021,** *(in press)*.
11. Kazmier, K.; Sharma, S.; Quick, M.; Islam, S. M.; Roux, B.; Weinstein, H.; Javitch, J. A.; McHaourab, H. S., Conformational dynamics of ligand-dependent alternating access in LeuT. *Nat Struct Mol Biol* **2014,** *21*, 472-479.
12. Garaeva, A. A.; Slotboom, D. J., Elevator-type mechanisms of membrane transport. Biochem. Soc. Trans **2020,** *48*, 1227-1241.
13. Hirschi, M.; Johnson, Z. L.; Lee, S. Y., Visualizing multistep elevator-like transitions of a nucleoside transporter. *Nature* **2017,** *545*, 66-70.
14. Sun, M.; Zheng, Q., Key Factors in Conformation Transformation of an Important Neuronic Protein Glucose Transport 3 Revealed by Molecular Dynamics Simulation. *ACS Chem Neurosci* **2019,** *10*, 4444-48.
15. Jardetzky, O., Simple allosteric model for membrane pumps. *Nature* **1966,** *211*, 969-70.
16. Quistgaard, E. M.; Löw, C.; Moberg, P.; Trésaugues, L.; Nordlund, P., Structural basis for substrate transport in the GLUT-homology family of monosaccharide transporters. *Nat Struct Mol Biol* **2013,** *20*, 766-8.
17. Keller, K.; Strube, M.; Mueckler, M., Functional expression of the human HepG2 and rat adipocyte glucose transporters in Xenopus oocytes. Comparison of kinetic parameters. *J Biol Chem* **1989,** *264*, 18884-18889.
18. Palfreyman, R. W.; Clark, A. E.; Denton, R. M.; Holman, G. D.; Kozka, I. J., Kinetic resolution of the separate GLUT1 and GLUT4 glucose transport activities in 3T3-L1 cells. *Biochem J* **1992,** *284*, 275-282.
19. Jensen, M. Ø.; Yin, Y.; Tajkhorshid, E.; Schulten, K., Sugar transport across lactose permease probed by steered molecular dynamics. *Biophys J* **2007,** *93*, 92-102.
20. Wambo, T. O.; Chen, L. Y.; Phelix, C.; Perry, G., Affinity and path of binding xylopyranose unto E. coli xylose permease. *Biochem Biophys Res Comm* **2017,** *494*, 202-206.

21. Liang, H.; Bourdon, A. K.; Chen, L. Y.; Phelix, C. F.; Perry, G., Gibbs free-energy gradient along the path of glucose transport through human glucose transporter 3. *ACS Chem Neuro* **2018,** *9*, 2815-2823.
22. Fu, X.; Zhang, G.; Liu, R.; Wei, J.; Zhang-Negrerie, D.; Jian, X.; Gao, Q., Mechanistic Study of Human Glucose Transport Mediated by GLUT1. *J Chem Inf Model* **2016,** *56*, 517-526.
23. Pan, Y.; Zhang, Y.; Gongpan, P.; Zhang, Q.; Huang, S.; Wang, B.; Xu, B.; Shan, Y.; Xiong, W.; Li, G.; Wang, H., Single glucose molecule transport process revealed by force tracing and molecular dynamics simulations. *Nanoscale Horiz* **2018,** *3*, 517-524.
24. Chen, L. Y.; Phelix, C. F., Extracellular gating of glucose transport through GLUT 1. *Biochem Biophys Res Comm* **2019,** *511*, 573-578.
25. Park, M. S., Molecular dynamics simulations of the human glucose transporter GLUT1. *PloS one* **2015,** *10*, e0125361.
26. Galochkina, T.; Ng Fuk Chong, M.; Challali, L.; Abbar, S.; Etchebest, C., New insights into GluT1 mechanics during glucose transfer. *Sci Rep* **2019,** *9*, 998.
27. Deng, D.; Xu, C.; Sun, P.; Wu, J.; Yan, C.; Hu, M.; Yan, N., Crystal structure of the human glucose transporter GLUT1. *Nature* **2014,** *510*, 121-125.
28. Jo, S.; Kim, T.; Iyer, V. G.; Im, W., CHARMM-GUI: a web-based graphical user interface for CHARMM. *J Comput Chem* **2008,** *29*, 1859-65.
29. Phillips, J. C.; Braun, R.; Wang, W.; Gumbart, J.; Tajkhorshid, E.; Villa, E.; Chipot, C.; Skeel, R. D.; Kale, L.; Schulten, K., Scalable molecular dynamics with NAMD. *J Comput Chem***2005,** *26*, 1781-802.
30. Huang, J.; MacKerell Jr, A. D., CHARMM36 all-atom additive protein force field: Validation based on comparison to NMR data. *J Comput Chem* **2013,** *34*, 2135-2145.
31. MacKerell, A. D.; Bashford, D.; Bellott; Dunbrack, R. L.; Evanseck, J. D.; Field, M. J.; Fischer, S.; Gao, J.; Guo, H.; Ha, S.; Joseph-McCarthy, D.; Kuchnir, L.; Kuczera, K.; Lau, F. T. K.; Mattos, C.; Michnick, S.; Ngo, T.; Nguyen, D. T.; Prodhom, B.; Reiher, W. E.; Roux, B.; Schlenkrich, M.; Smith, J. C.; Stote, R.; Straub, J.; Watanabe, M.; Wiórkiewicz-Kuczera, J.; Yin, D.; Karplus, M., All-Atom Empirical Potential for Molecular Modeling and Dynamics Studies of Proteins†. *J Phys Chem B* **1998,** *102*, 3586-3616.
32. Jorgensen, W. L.; Chandrasekhar, J.; Madura, J. D.; Impey, R. W.; Klein, M. L., Comparison of Simple Potential Functions for Simulating Liquid Water. *J Chem Phys* **1983,** *79*, 926-935.
33. Feller, S. E.; Zhang, Y. H.; Pastor, R. W.; Brooks, B. R., Constant-Pressure Molecular-Dynamics Simulation - the Langevin Piston Method. *J Chem Phys* **1995,** *103*, 4613-4621.
34. Darden, T.; York, D.; Pedersen, L., Particle Mesh Ewald - an N.Log(N) Method for Ewald Sums in Large Systems. *J Chem Phys* **1993,** *98*, 10089-10092.
35. Verlet, L., Computer Experiments on Classical Fluids .I. Thermodynamical Properties of Lennard-Jones Molecules. *Phys Rev* **1967,** *159*, 98.
36. Miyamoto, S.; Kollman, P. A., SETTLE - an analytical version of the Shake and Rattle algorithm for rigid water models. *J Comput Chem* **1992,** *13*, 952-962.
37. Tuckerman, M.; Berne, B. J.; Martyna, G. J., Reversible multiple time scale molecular-dynamics. *J Chem Phys* **1992,** *97*, 1990-2001.
38. Smart, O. S.; Neduvelil, J. G.; Wang, X.; Wallace, B. A.; Sansom, M. S. P., HOLE: A program for the analysis of the pore dimensions of ion channel structural models. *J Mol Graphics* **1996,** *14*, 354-360.
39. Iglesias-Fernandez, J.; Quinn, P. J.; Naftalin, R. J.; Domene, C., Membrane phase-dependent occlusion of intramolecular GLUT1 cavities demonstrated by simulations. *Biophys J* **2017,** *112*, 1176-1184.

40. Karshikoff, A.; Nilsson, L.; Ladenstein, R., Rigidity versus flexibility: the dilemma of understanding protein thermal stability. *FEBS J* **2015,** *282*, 3899-917.
41. Fu, X.; Zhang, G.; Liu, R.; Wei, J.; Zhang-Negrerie, D.; Jian, X.; Gao, Q., Mechanistic study of human glucose transport mediated by GLUT1. *J Chem Inf Model* **2016,** *56*, 517-26.
42. Holyoake, J.; Caulfeild, V.; Baldwin, S. A.; Sansom, M. S. P., Modeling, Docking, and Simulation of the Major Facilitator Superfamily. *Biophys J* **2006,** *91*, L84-L86.
43. Barnett, J. E.; Holman, G. D.; Chalkley, R. A.; Munday, K. A., Evidence for two asymmetric conformational states in the human erythrocyte sugar-transport system. *Biochem J* **1975,** *145*, 417-429.
44. Naftalin, R. J., Osmotic Water Transport with Glucose in GLUT2 and SGLT. *Biophys J* **2008,** *94*, 3912-3923.
45. MacAulay, N.; Zeuthen, T., Water transport between CNS compartments: contributions of aquaporins and cotransporters. *Neurosci* **2010,** *168*, 941-56.
46. Sussman, J. L.; Silman, I., Computational studies on cholinesterases: Strengthening our understanding of the integration of structure, dynamics and function. *Neuropharm* **2020,** *179*, 108265.
47. Hresko, R. C.; Kraft, T. E.; Quigley, A.; Carpenter, E. P.; Hruz, P. W., Mammalian Glucose Transporter Activity Is Dependent upon Anionic and Conical Phospholipids. *J Biol Chem* **2016,** *291*, 17271-17282.
48. Selvam, B.; Yu, Y.-C.; Chen, L.-Q.; Shukla, D., Molecular Basis of the Glucose Transport Mechanism in Plants. *ACS Central Sci* **2019,** *5*, 1085-1096.
49. Cheng, K. J.; Selvam, B.; Chen, L.-Q.; Shukla, D., Distinct Substrate Transport Mechanism Identified in Homologous Sugar Transporters. *J Phys Chem B* **2019,** *123*, 8411-8418.
50. Nussinov, R.; Tsai, C.-J., Allostery without a conformational change? Revisiting the paradigm. *Curr Opin Struct Biol* **2015,** *30*, 17-24.
51. Motlagh, H. N.; Wrabl, J. O.; Li, J.; Hilser, V. J., The ensemble nature of allostery. *Nature* **2014,** *508*, 331-339.
52. Quinn, P. J., Principles of membrane stability and phase behavior under extreme conditions. *J Bioenergetics Biomem* **1989,** *21*, 3-19.
53. Schneider, M. F.; Marsh, D.; Jahn, W.; Kloesgen, B.; Heimburg, T., Network formation of lipid membranes: triggering structural transitions by chain melting. Proc Natl Acad Sci U S A. **1999,** *96*, 14312-14317.
54. Owen, J. D.; Solomon, A. K., Control of nonelectrolyte permeability in red cells. Biochim. Biophys. Acta **1972,** *290*, 414-8.
55. Macey, R. L.; Farmer, R. E. L., Inhibition of water and solute permeability in human red cells. *BBA Biomembranes* **1970,** *211*, 104-106.
56. Fischbarg, J.; Kuang, K. Y.; Vera, J. C.; Arant, S.; Silverstein, S. C.; Loike, J.; Rosen, O. M., Glucose transporters serve as water channels. Proc Natl Acad Sci U S A. **1990,** *87*, 3244-3247.
57. Iserovich, P.; Wang, D.; Ma, L.; Yang, H.; Zuniga, F. A.; Pascual, J. M.; Kuang, K.; De Vivo, D. C.; Fischbarg, J., Changes in glucose transport and water permeability resulting from the T310I pathogenic mutation in Glut1 are consistent with two transport channels per monomer. *J Biol Chem* **2002,** *277*, 30991-7.
58. Liu, Z.; Sanchez, M. A.; Jiang, X.; Boles, E.; Landfear, S. M.; Rosen, B. P., Mammalian glucose permease GLUT1 facilitates transport of arsenic trioxide and methylarsonous acid. *Biochem Biophys Res Comm* **2006,** *351*, 424-430.

59. Barnett, C. B.; Naidoo, K. J., Ring Puckering: A metric for evaluating the accuracy of AM1, PM3, PM3CARB-1, and SCC-DFTB carbohydrate QM/MM simulations. *J Phys Chemy B* **2010,** *114*, 17142-17154.
60. Hamill, S.; Cloherty, E. K.; Carruthers, A., The Human Erythrocyte Sugar Transporter Presents Two Sugar Import Sites. *Biochemistry* **1999,** *38*, 16974-16983.
61. Wong, H. Y.; Law, P. Y.; Ho, Y. Y., Disease-associated Glut1 single amino acid substitute mutations S66F, R126C, and T295M constitute Glut1-deficiency states in vitro. *Mol Genet Metab* **2007,** *90*, 193-8.
62. Cunningham, P.; Afzal-Ahmed, I.; Naftalin, R. J., Docking studies show that D-glucose and quercetin slide through the transporter GLUT1. *J Biol Chem* **2006,** *281*, 5797-803.
63. Lacko, L.; Burger, M., Interaction of some disaccharides with the carrier system for aldoses in erythrocytes. *Biochem J* **1962,** *83*, 622-625.
64. Levine, M.; Oxender, D. L.; Stein, W. D., The substrate-facilitated transport of the glucose carrier across the human erythrocyte membrane. *BBA Biophys* **1965,** *109* , 151-163.
65. Miller, D. M., The kinetics of selective biological transport: III. Erythrocyte-monosaccharide transport data. *Biophys J* **1968,** *8*, 1329-1338.
66. Miller, D. M., The kinetics of selective biological transport: V. Further data on the erythrocyte-monosaccharide transport system. *Biophys J* **1971,** *11*, 915-923.
67. Naftalin, R. J., Evidence from temperature studies that the human erythrocyte hexose transporter has a transient memory of its dissociated ligands. *Exp Physiol* **1998,** *83*, 253-8.
68. McAllister, M. S.; Krizanac-Bengez, L.; Macchia, F.; Naftalin, R. J.; Pedley, K. C.; Mayberg, M. R.; Marroni, M.; Leaman, S.; Stanness, K. A.; Janigro, D., Mechanisms of glucose transport at the blood-brain barrier: an in vitro study. *Brain Res* **2001,** *904*, 20-30.
69. Simpson, I. A.; Carruthers, A.; Vannucci, S. J., Supply and demand in cerebral energy metabolism: the role of nutrient transporters. J. Cereb. Blood Flow Metab **2007,** *27*, 1766-91.
70. Deng, D.; Sun, P. C.; Yan, C. Y.; Ke, M.; Jiang, X.; Xiong, L.; Ren, W. L.; Hirata, K.; Yamamoto, M.; Fan, S. L.; Yan, N., Molecular basis of ligand recognition and transport by glucose transporters. *Nature* **2015,** *526*, 391.
71. Yan, N., A Glimpse of Membrane Transport through Structures-Advances in the Structural Biology of the GLUT Glucose Transporters. *J Mol Biol* **2017,** *429*, 2710-2725.
72. Chen, X.; Zhao, Y.; Lyu, S.; Gao, G.; Gao, Y.; Qi, Y.; Du, J., Identification of novel inhibitors of GLUT1 by virtual screening and cell-based assays. *Invest New Drugs* **2021**.